

Research Paper

Rapid *In Situ* MRI Traceable Gel-forming Dual-drug Delivery for Synergistic Therapy of Brain Tumor

Feng-Wei Lin^{1*}, Pin-Yuan Chen^{2*}, Kuo-Chen Wei³, Chiung-Yin Huang³, Chih-Kuang Wang⁴, Hung-Wei Yang¹✉

1. Institute of Medical Science and Technology, National Sun Yat-sen University, Kaohsiung 80424, Taiwan;
2. Department of Neurosurgery, Chang Gung Memorial Hospital, Keelung 20401, Taiwan; School of Medicine, Chang Gung University, Taoyuan 33302, Taiwan;
3. Department of Neurosurgery, Linkou Chang Gung Memorial Hospital, Taoyuan 33305, Taiwan. School of Medicine, Chang Gung University, Taoyuan 33302, Taiwan;
4. Department of Medicinal and Applied Chemistry, Kaohsiung Medical University, Kaohsiung 80708, Taiwan.

* These authors contributed equally.

✉ Corresponding author: Tel.: +886-7-5252000x5842; fax: +886-7-5250151 E-mail address: howardyang@mail.nsysu.edu.tw

© Ivyspring International Publisher. This is an open access article distributed under the terms of the Creative Commons Attribution (CC BY-NC) license (<https://creativecommons.org/licenses/by-nc/4.0/>). See <http://ivyspring.com/terms> for full terms and conditions.

Received: 2017.02.28; Accepted: 2017.04.21; Published: 2017.06.25

Abstract

Preventing tumor recurrence after surgical resection of a brain tumor is a significant clinical challenge because current methods deliver chemotherapeutic agents in a rapid manner and are not effective against the residual tumor cells. To overcome this drawback, we report a simple method to prepare magnetic resonance imaging (MRI) traceable ultra-thermosensitive hydrogels with rapid gelation ability from aqueous solution within 4 s at 28 °C for hydrophilic (epirubicin, EPI) and hydrophobic (paclitaxel, PTX) drugs co-delivery with bovine serum albumin nanoparticles (BSA NPs) incorporation. The results showed the average survival of gliosarcoma-bearing (MBR 614 or U87) mice receiving BSA/PTX NPs incorporated hydrogel_{Ed}/EPI increased to 63 days or 69 days with no tumor recurrence observed. Our synergistic strategy presents a new approach to the development of a local drug delivery system for the prevention of brain tumor recurrence.

Key words: Thermosensitivity hydrogels, MRI traceability, sustained drug release, tumor recurrence, brain tumor.

Introduction

About 40,000 people are diagnosed with primary brain tumors in the United States each year, an estimated 15,000 have glioblastoma multiforme (GBM), which is still associated with poor prognosis with 14.6 month of median survival after surgical resection combined with chemotherapy and radiation [1, 2]. The blood-brain barrier (BBB) is the major obstruction for chemotherapy to treat brain tumor, about 98% of small molecule drug and almost 100% of large molecule drugs do not penetrate the BBB [3]. The receptor-mediated nanocarriers with chemotherapeutics loading have been prepared for transport across the BBB [4, 5], but the concentration of particles that enter the brain is still not sufficient via i.v. administration. Another approach is to bypass the

BBB: BCNU-impregnated biodegradable polymer wafers (i.e., Gliadel[®]) which slowly release BCNU over a prolonged period have provided a novel approach to circumvent the systemic toxicity and has been particularly successful in improving the survival [1, 6, 7]. However, the inhibition efficacy may be limited because of the penetration depth into tissue of BCNU released from the wafers is about 1 mm [8]. Currently, a new technique using focused ultrasound (FUS) in the presence of circulating microbubbles (MBs) was used to locally, temporarily and noninvasively open the BBB for enhancing the local concentration of therapeutic agents in the brain tumor [9, 10], but it has a risk of bleeding by hardly choosing suitable power of FUS for each patient. Thus, an

alternate approach is convection-enhanced delivery (CED), in which the chemotherapeutics are infused into the brain under a positive pressure gradient to overcome the obstruction of BBB. But the CED along is not sufficient to significantly increase the survival because of the most chemotherapeutics have short half-life time in the brain resulted in they disappear soon after the infusion stops [11].

Hydrogels have become popular drug delivery vehicles and been the best candidates for locally controlled drug release because of their high water content, highly tunable mechanical properties, low systemic toxicity, and side effects [12, 13]. Hydrogels can undergo three-dimensional structural changes in response to pH [14], temperature [15], light [16], and electrical fields [17], which the temperature-sensitive hydrogels are the most commonly studied among the environmentally sensitive polymer-based hydrogels in controlled drug release research. Thus, we propose a strategy to inhibit tumor growth and prevent tumor recurrence by applying the drug-loaded hydrogels on the residual tumor tissues after surgical resection. However, most of temperature-sensitive hydrogels cannot solidified immediately gel from solution phase in the post-operated tissues because of their lower critical solution temperature (LCST) at around the body temperature (34-37°C) [18, 19], such as OncoGel™, a non-Cremophor based formulation of PTX in ReGel, was designed for local delivery of PTX to solid tumors. ReGel polymers transition from a free-flowing water soluble low viscosity solution at room temperatures to a viscous, water insoluble biodegradable controlled-release gel at body temperature (35-37°C) that may cause the failure of tumor inhibition [20].

To realize the strategy, two key issues have to be overcome: (i) the LCST should be lower than 30°C that allow the gelation of hydrogel in the operation room; (ii) the gelation time in tissues should be short as possible; (iii) the gel should be traceable by molecular imaging. Thus, in this study, the rapid gelation and magnetic resonance imaging (MRI) traceable hydrogels with low LCST (26-28°C) were developed by blending negative charged carboxymethyl cellulose (CMC)-grafted poly(*N*-isopropylacrylamide-co-methacrylic acid) (CMC-g-PNIPAAmMA) and positive charged gadopentetic acid/branched polyethylenimine (DTPA_{Gd}/bPEI) to form hydrogel_{Gd} which could be used to deliver hydrophilic epirubicin (EPI) and hydrophobic paclitaxel (PTX) with bovine serum albumin nanoparticles (BSA NPs) incorporation. Besides, the hydrogel_{Gd} also exhibited excellent magnetic resonance (MR) T1 contrast ability for real-time imaging monitor of hydrogel_{Gd} distribution and degradation (Figure 1A). Our studies

showed this ultra-thermosensitive hydrogel could be congealed in 4 sec at 28°C (Table S1) and the use of this hydrogel_{Gd} containing EPI and PTX can significantly inhibit tumor growth of gliosarcoma challenge in a mouse model (Figure 1B). Although the PNIPAAm-based hydrogel has studied well, no one significantly reduced its LCST and gave it multi-functional ability using such simple method.

Methods

Synthesis of amine-terminated carboxymethyl cellulose

The amine-terminated carboxymethyl cellulose (amine-terminated CMC) was prepared by conjugating the ethylenediamine dihydrochloride (EDA; Sigma-Aldrich, St. Louis, MO) to the CMC. Briefly, CMC (0.5 g) was firstly dissolved in 100 mL of deionized (DI)-water then 3.2 g of EDA was added into the solution at pH 6.5 (solution I). Next, the 0.8 g of 1-ethyl-3-(3-dimethylaminopropyl) carbodiimide (EDC; Sigma-Aldrich, St. Louis, MO) and 0.7 g of 1H-1,2,3-benzotriazol-1-ol (HOBt; Sigma-Aldrich, St. Louis, MO) were dissolved in 5 mL 50 % DMSO solution (solution II). The solution I and solution II were mixed together and stirred at room temperature for 24 h in the dark, the solution was then put into Spectra/Por 3 dialysis membrane with molecular weight cutoff of 3,500 Da and purified by DI-water to remove the unreacted chemicals. The purified solution was then lyophilized to obtain the amine-terminated carboxymethyl cellulose powders.

Synthesis of CMC-modified PNIPAAmMA

One hundred milligram of poly(*N*-isopropylacrylamide-co-methacrylic acid) (PNIPAAmMA; 60 kDa, Sigma-Aldrich, St. Louis, MO) was dissolved in 10 mL of 0.5 M MES buffer (pH 5.5) then 98 mg of EDC and 104 mg of *N*-Hydroxysuccinimide (NHS; Sigma-Aldrich, St. Louis, MO) were further added into the solution and reacted at 10°C for 1.5 h in the dark to activate the carboxylic groups of PNIPAAmMA. Ten milliliter of amine-terminated CMC (20 mg) was mixed with above solution at 10°C and reacted for 3.5 h in the dark. The product was precipitated at 50°C, followed by centrifugation (15,000 rpm; 2 min) and resuspension in DI-water. To remove unreacted components, the solution was exhaustively dialyzed (MWCO 10,000; Spectra/Por® Dialysis Membrane) against DI-water at 4°C for 2 days.

Preparation of MRI traceable hydrogels

To prepare the rapid gelation and MRI traceable hydrogels, the DTPA_{Gd} was first modified with bPEI to form positive charged DTPA_{Gd}/bPEI. Briefly, the

DTPA_{Gd} was dissolved in 0.2 mL (100 mg/mL) 0.5 M MES buffer (pH 5.5) then 48 mg of EDC and 54 mg of NHS were further added into the solution and reacted at room temperature for 30 min in the dark to activate the carboxylic groups of DTPA_{Gd}. The bPEI (M_w: 800) was further reacted with above solution at room temperature for 3 h in the dark to form DTPA_{Gd}/bPEI. Finally, the synthesized CMC-modified

PNIPAAmMA was mixed with DTPA_{Gd}/bPEI (DTPA_{Gd}/bPEI/CMC-modified PNIPAAmMA = 1/2 or 1/5; wt/wt) for 1 h at 4°C. The hydrogels were precipitated at 50°C, followed by centrifugation (15,000 rpm; 2 min) and resuspension in DI-water. The obtained highly thermosensitive hydrogel_{Gd} was kept at 4°C for further use.

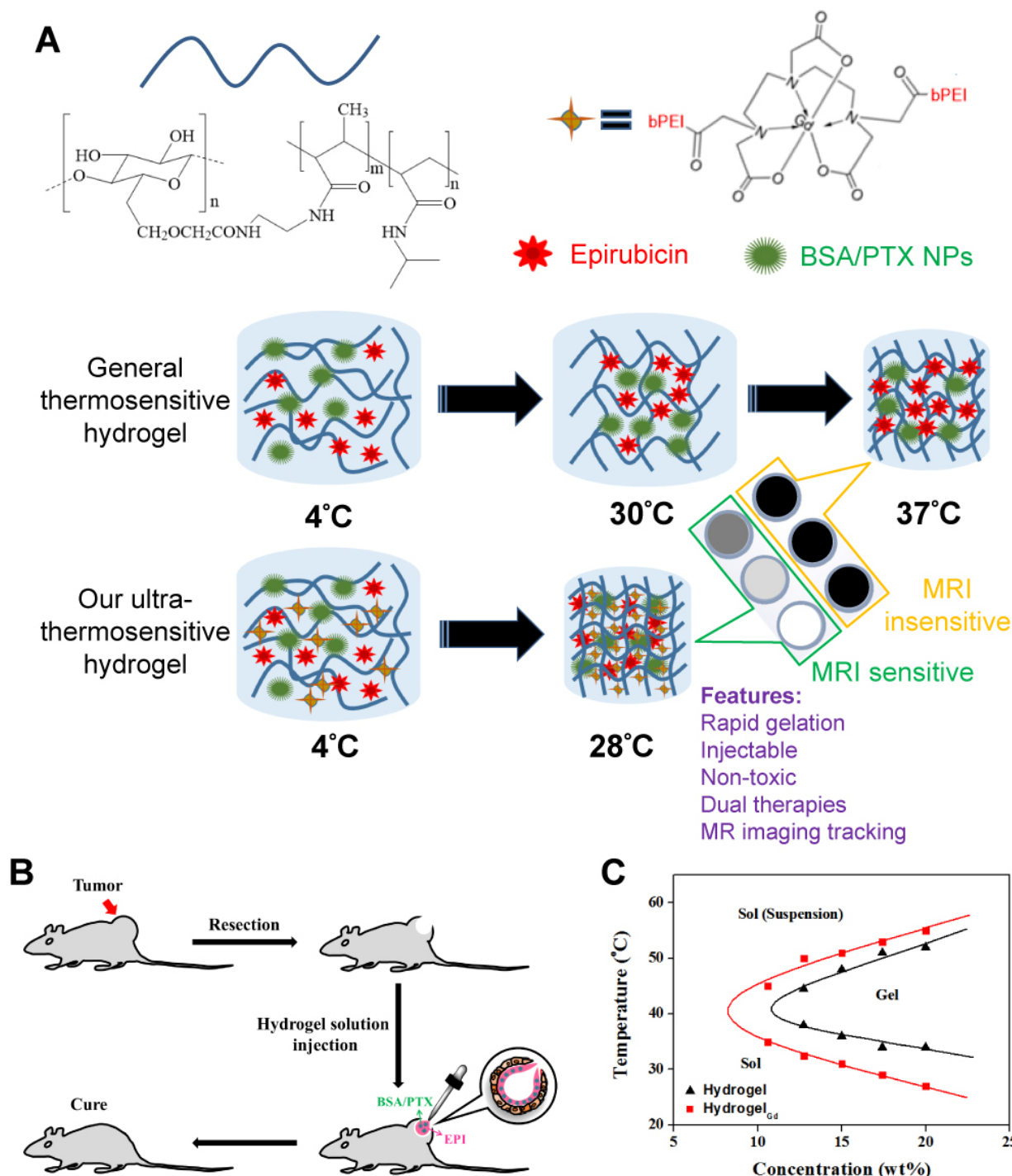


Figure 1. (A) Schematic description of BSA/PTX NPs incorporated hydrogel/EPI and BSA/PTX NPs incorporated hydrogel_{Gd}/EPI formation at different temperatures. (B) Schematic representation of BSA/PTX NPs incorporated hydrogel_{Gd}/EPI implantation after surgical operation for local tumor inhibition and recurrence prevention. (C) The sol-gel phase transition diagram of hydrogel and hydrogel_{Gd}.

Phase transition characterizations

To investigate the influence of polymer concentration and presence of DTPA_{Gd}/bPEI on the thermally induced morphological change during 4°C and 37°C, the hydrogel and hydrogel_{Gd} solutions were prepared with different polymer concentrations by dissolving the solutes in DI-water. The phase transition property of each test sample was investigated using a differential scanning calorimeter (DSC; Q20, TA Instruments, New Castle, DE). After equilibration at 4°C for 1 h, the solutions (20 wt%) were hermetically sealed in aluminum pans for DSC experiments. Programmed heating was carried out at 2°C/min in the temperature range from 20 to 45°C, under a nitrogen gas flow. The lower critical solution temperature (LCST) was determined as the onset point of the endothermic peak [21].

The melting temperature (T_m) of each test sample was also investigated using the DSC. Twenty milligram of hydrogel or hydrogel_{Gd} was lyophilized to be powder then was hermetically sealed in aluminum pans for DSC experiments. Programmed heating was carried out at 2°C/min in the temperature range from 10 to 80°C, under a nitrogen gas flow. The T_m was determined as the onset point of the endothermic peak.

Swelling measurements

For several applications, in particular in the medical and pharmaceutical fields, the swelling behavior of the hydrogels was investigated in DI water. The effect of temperature of the swelling medium on the equilibrium water uptake of the hydrogel samples was determined at different temperature (20-60 °C) and removed from water at regular time intervals. The percent mass swelling was determined using the following expression:

$$\text{Swelling \%} = \frac{M_t - M_0}{M_0}$$

where M_0 and M_t are the initial mass and mass at different time-intervals, respectively.

Synthesis of BSA/PTX NPs

The BSA/PTX NPs were prepared as previously described using a desolvation method [22]. Briefly, 20 mg of BSA was first dissolved in 2 mL of DI-water containing 10 mM of NaCl, then 0.2 mL of different concentrations of PTX was added into above solution and stirred for 30 min at room temperature. For desolvation, the 95% ethanol was dropped into the solution with a constant rate of 0.3 mL/min under magnetic stirring (500 rpm) at room temperature till the solution became turbid. To stabilize BSA/PTX NPs, the turbid solution was stirred continuously for

30 min without further addition of ethanol. After that, the as-prepared BSA/PTX NPs were denatured at 70°C for 30 min to solidify the NPs. The BSA/PTX NPs were then centrifuged and washed with DI-water to remove ethanol.

The untrapped PTX in the supernatant was examined by high performance liquid chromatography (HPLC; Hitachi L-2000, Hitachi, Japan) to calculate the drug encapsulation and loading efficiency. PTX was analysed by HPLC on a SUPELCO SİLTM LC-18 column (4.6 x 250 mm) using an L-2130 pump and an L-2400 UV-detector. The mobile phase of the HPLC was a 40:60 (v/v) mixture of DI water and acetonitrile with a flow rate of 2 mL/min; data were measured at 227 nm and quantitatively determined by comparing with a standard curve.

In vitro hemolysis test

Hemolytic activity of BSA NPs incorporated hydrogel_{Gd} was tested by direct contact methods according to ISO 10 993-5 1992 [23]. Anticoagulated rat blood (0.02 mL) was added to 1 ml of physiological saline buffer (PBS) containing different concentrations of BSA NPs incorporated hydrogel_{Gd} or PBS as negative control or DI-water as positive control. Then the contents of the tubes were gently mixed and placed in incubator at 37°C. After incubation for 3 h, the samples were centrifuged at 1,000 rpm for 10 min and absorbance of the supernatant of each tube was measured by ultraviolet-visible spectroscopy (UV-vis; V750, JASCO, Easton, MD) at 545 nm. The rate of hemolysis was calculated according to the following equation:

$$\text{Hemolysis (\%)} = \frac{\text{OD}_{\text{sample}} - \text{OD}_{\text{negative}}}{\text{OD}_{\text{positive}} - \text{OD}_{\text{negative}}} \times 100$$

Drug entrapment in hydrogel_{Gd}

To evaluate the drug encapsulation levels in hydrogel_{Gd}, the hydrogel_{Gd} solution (20 wt%) was prepared by dissolving the polymer in DI-water then mixed with different concentrations of EPI (80-600 µg) and BSA/PTX NPs at 4°C for 30 min in vial, the vial was heated to 40°C to form BSA/PTX NPs incorporated hydrogel_{Gd}/EPI. One milliliter of PBS at 40°C was added into the vial to remove the untrapped EPI and BSA/PTX NPs on the supernatant. The supernatant was then centrifuged at 8000 rpm for 10 min to separate the EPI and BSA/PTX NPs. The separated BSA/PTX NPs were resuspended in 1% pepsin solution and reacted at 4°C for 30 min then centrifuged at 12,000 rpm for 10 min to obtain the PTX which was encapsulated in the BSA NPs. The concentration of extracted EPI and PTX were analysed by HPLC. EPI was analysed by HPLC on a

SUPELCO SILTM LC-18 column (4.6 x 250 mm) using an L-2130 pump and an L-2400 UV-detector. The mobile phase of the HPLC was a 50/15/35 (v/v/v) mixture of DI water, acetonitrile and methanol with a flow rate of 1.5 mL/min and data were collected at 256 nm and quantitatively determined by comparing with a standard curve.

In vitro release studies

The BSA/PTX NPs incorporated hydrogel_{Gd}/EPI sample was prepared in a vial and then 1 mL of PBS (pH 5.6) at 37°C was added into the vial and incubated at 37°C with reciprocal shaking (70 rpm) in a thermostatically controlled water bath for a time periods ranging from 1 h to 2 weeks. The supernatant was collected and analysed by HPLC. The supernatant was then centrifuged at 8,000 rpm for 10 min to separate the EPI and BSA/PTX NPs. The separated BSA/PTX NPs were resuspended in 1% pepsin solution and reacted at 4°C for 30 min then centrifuged at 12,000 rpm for 10 min to obtain the PTX which was encapsulated in the BSA NPs. The concentration of extracted EPI and PTX were calculated with respect to a calibration curve by HPLC.

MR phantoms of BSA NPs incorporated hydrogel_{Gd}

For *in vitro* measurements, pure DTPA_{Gd}/bPEI and BSA NPs incorporated hydrogel_{Gd} were diluted to different concentrations of DTPA_{Gd}/bPEI containing with physiological saline. Circular wells (inner diameter = 5 mm) were filled with 100 µL of contrast agent sample or physiological saline as control and were placed in the MR scanner (Clinscan, Bruker, Germany; 7T). Spin-lattice relaxivity maps were calculated from two T1-weighted images with different flip angles (gradient recalled echo sequence, TR/TE = 2.3 ms/0.76 ms, slice thickness = 0.8 mm, matrix = 132 x 192, and flip angle = 5°/20°). The correlation between R1 (= 1/T1) mapping and DTPA_{Gd}/bPEI concentration was determined.

In vivo MR imaging

For MR imaging, a 7-T MR scanner and a 4-channel surface coil was used. The mouse was placed in an acrylic holder, positioned in the center of the magnet, and anesthetized with isoflurane gas (1-2%) at 50-70 breaths/min during the entire MR imaging procedure. The distribution of BSA NPs incorporated hydrogel_{Gd} was investigated after implanting in residue tumor tissues after resection; the animals were relocated into the MR imaging scanning room for imaging after one week of implanting. Contrast-enhanced T1-weighted images with different flip angles were acquired to calculate

spin-lattice relaxivity maps by transferring two images with different flip angles (gradient recalled echo sequence, TR/TE = 2.3 ms/0.76 ms, slice thickness = 0.8 mm, slice number = 14, matrix = 132 x 192, and flip angle = 5°/20°).

In vitro cell studies

Human brain tumor cells (MBR 614 cell) were cultured in DMEM supplemented with 2.2 mg/mL sodium carbonate, 10% fetal bovine serum, 50 µg/mL gentamicin, 50 µg/mL penicillin, 50 µg/mL streptomycin, and 25 mM HEPES at 37°C and 5% CO₂. Approximately 10,000 cells (i.e., 150 µL of a suspension of 6.67 x 10⁴ cells/mL) were placed in each well of a 96-well culture plate and incubated in a humidified chamber at 37°C and 5% CO₂ for 24 h.

For the biocompatibility test of BSA NPs-incorporated hydrogel_{Gd} samples (30 µL) containing different concentrations of BSA NPs were added to each well, and incubation was continued for 24 h. Before counting, the culture medium was removed, and the cells were incubated in 120 µL of XTT solution for 2 h. Subsequently, 100 µL of the XTT solution was removed from each well and transferred to a 96-well counting dish. The biocompatibility of BSA NPs incorporated hydrogel_{Gd} was evaluated by measuring the OD at 490 nm using an ELISA reader.

For *in vitro* anti-proliferation test, 30 µL different concentrations of samples (free EPI, hydrogel_{Gd}/EPI, and BSA/PTX NPs incorporated hydrogel_{Gd}/EPI) were added to the wells, and incubation was continued for 24, 48 or 72 h. Before counting, the culture medium was removed, and the cells were incubated in 120 µL of XTT solution for 2 h. Subsequently, 100 µL of the XTT solution was removed from each well and transferred to a 96-well counting dish. The cytotoxicity toward MBR 614 cell cells *in vitro* was evaluated by measuring the OD at 490 nm using an ELISA reader.

To investigate the drug release by cell imaging, the MBR 614 cells were seeded in a density of 20,000 cells/well (i.e., 300 µL of a suspension of 6.67 x 10⁴ cells/mL) in a 24-well plate. After 24 h of cell attachment, the wells were carefully washed with PBS at 37°C followed by the addition of 30 µL of different samples (i.e., free EPI, hydrogel_{Gd}/EPI, and BSA/FITC incorporated hydrogel_{Gd}/EPI) for upto 8 h. Next, the cells were washed twice with ice cold PBS (pH = 7.4) to remove the residual samples, fixed with fresh ice ethanol for 5 min at room temperature. Cells were washed three times with HBSS then their nuclei were stained by Hoechst. The distribution of EPI and BSA/FITC NPs in cells was analyzed by inverted fluorescent microscopy (Eclipse Ti-S, Nikon, Melville, NY).

Anti-active caspase-3 staining

The skin tissues of mice with or without the treatment of BSA NPs incorporated hydrogel_{Gd} were placed in 4% PFA and paraffin embedded were cut into sections of 4 μ m thickness. The immunohistochemistry was performed with the Quanto Detection System HRP (Thermo Fisher Scientific, Inc., Fremont, CA, USA); the sections were incubated with antigen retrieval solution pH 6.0, then blocked with endogenous peroxidase Ultra V Block for 10 min. (Thermo Fisher Scientific). Next, the sections were incubated with UltraVision protein block (Thermo Fisher Scientific) for 5 min to reduce nonspecific background. Apoptosis staining was detected using anti-active caspase 3 antibody (1:500, BD #559565) incubated at 4°C overnight; and then the signaling was amplified using the Primary Antibody Amplifier Quanto (Thermo Fisher Scientific) for 10 minutes. Then, the secondary antibody (HRP Polymer Quanto) was added for 10 minutes. Finally, the DAB chromogen was added for 5 min and counterstained with Mayer's hematoxylin(DAKO) then examined under a light microscope.

In vivo anti-proliferation studies

All animal experiments were approved by the Institutional Animal Care and Use Committee of Chang Gung University and performed in accordance with their guidelines. Mice were raised in a room with a thermostat at 26°C. The C57BL/6 and Nu/Nu mice weighing ~25-30 g (5-6 weeks old) were tested to confirm the efficacy of the proposed approach. Hypodermic brain tumors were induced in 24 mice (MBR 614 cells) and 30 mice (U87 cells). Briefly, cultured MBR 614 or U87 tumor cells (2×10^6 cells/mouse) were injected over a 2-min period into the hypoderm using a syringe, and needle-withdrawal was carried out over another period of 0.5 min.

Experiments were performed with four groups of mice bearing MBR 641-2 tumors (n = 6). To fit the standard clinical treatment strategy, all mice received tumor resection. Half of tumor was resected while the tumors grew up to around 200 mm³. Control mice received no further treatment after tumor resection. The second group received a single dose of pure EPI (6 mg/kg) via the external jugular vein after tumor resection. The BSA NPs incorporated hydrogel_{Gd} and BSA/PTX NPs incorporated hydrogel_{Gd}/EPI (containing 1 mg of EPI and 0.1 mg of PTX) were implanted to the residual tumor tissues for third and fourth groups after tumor resection.

Experiments were performed with five groups of mice bearing U87 tumors (n = 6). To fit the standard clinical treatment strategy, all mice received tumor

resection. Half of tumor was resected while the tumors grew up to around 200 mm³. Control mice received no further treatment after tumor resection. The BSA NPs incorporated hydrogel_{Gd}, hydrogel_{Gd}/EPI, BSA/PTX NPs incorporated hydrogel_{Gd}, and BSA/PTX NPs incorporated hydrogel_{Gd}/EPI (containing 1 mg of EPI and 0.1 mg of PTX) were implanted to the residual tumor tissues for second, third, fourth, and fifth groups after tumor resection.

For ethical reasons, animals were euthanized when the volume of the tumor reached to 3 cm³, which was defined as survival time. The tumor volume was calculated as: tumor volume (V) = length \times width \times width/2 [24].

Results and Discussion

The general thermosensitive hydrogels (LCST \geq 32°C) were not able to be used for *in situ* drug delivery after surgical resection due to the temperature of operating room (always below 30°C) is always higher than the LCST of general hydrogels that would cause the failure of gel-forming in tissues. Thus, this study proposed a utility of *in situ* MRI traceable dual-drug delivery system which can rapid gelation (LCST \leq 28°C) in tissues for preventing the post-operative recurrence of brain tumor.

Characterization of the hydrogels

PNIPAAm is a biocompatible but not biodegradable biopolymer, and, thus, its use raises concerns of side-effect [25]. By grafting bioerodible materials can provide enhanced patient compliance and minimize undesirable tissue reactions following drug administration (i.e., gelatin) [26, 27]. Thus, we grafted the CMC to the polymer chains of PNIPAAmMA forming CMC-g-PNIPAAmMA (also call hydrogel) for increasing the biodegradability (Figure S1). The presence of CMC in CMC-g-PNIPAAmMA was confirmed by Fourier transform infrared spectroscopy (FTIR). The characteristic bands present in PNIPAAmMA are C=O stretching vibration (amide I) at 1650 cm⁻¹, and N-H binding vibration (amide II) band at 1542 cm⁻¹ and C=O stretching vibration (carboxyl) at 1723 cm⁻¹ [28]. After grafting of CMC, additional peaks corresponding to O-C-O group as bridge between glucose chains (1134 cm⁻¹) and ether group (CH₂-O-CH₂; 1040 cm⁻¹) for amine-terminated CMC (Figure S2) [29]. By mixing with DTPA_{Gd}/bPEI, the LCST of formed hydrogel_{Gd} was decreased to 26.2°C from 34.8°C at a 20 wt% of CMC-g-PNIPAAmMA (Figure 1C) that confirmed by differential scanning calorimeter (DSC) thermograms (Figure S3A) due to the negative charged molecule chains of

CMC-g-PNIPAAmMA (-26.4 ± 1.4 mV) interacted with the positive charged DTPA_{Gd}/bPEI (33.6 ± 4.2 mV) to make the polymer chains more compact, so caused decreasing the temperature of phase transition and increasing the melting temperature (from 56.2°C to 64.6°C; Figure S3B). Both the hydrogel (20 wt%) and hydrogel_{Gd} (20 wt%) exhibited free-flowing sol phase at 4°C, only hydrogel_{Gd} became opaque free-flowing sol phase at 20°C then rapidly changed to non-flowing gel phase while the temperature increased to 28°C. Conversely, the hydrogel has to be incubated at 37°C for phase transition to non-flowing gel phase. We also did the swelling studies (Figure S4), the hydrogel (CMC-modified PNIPAAmMA)

became more compact by mixing with DTPA_{Gd}/bPEI that let the swelling ration of the hydrogel decreased, which is due to decrease of pore size. Below the LCST, the CMC-modified PNIPAAmMA swells, above the LCST it becomes opaque white (Figure 2A). After heating hydrogel_{Gd} solution to 28°C, the significant gel forming and the EPI and FITC-labeled BSA NPs were indeed entrapped in the hydrogel_{Gd} to show the red and green fluorescence (Figure 2B). The results demonstrated the potential application of the prepared hydrogel_{Gd} for simultaneous *in situ* co-delivery of hydrophilic and hydrophobic drugs after surgical operation.

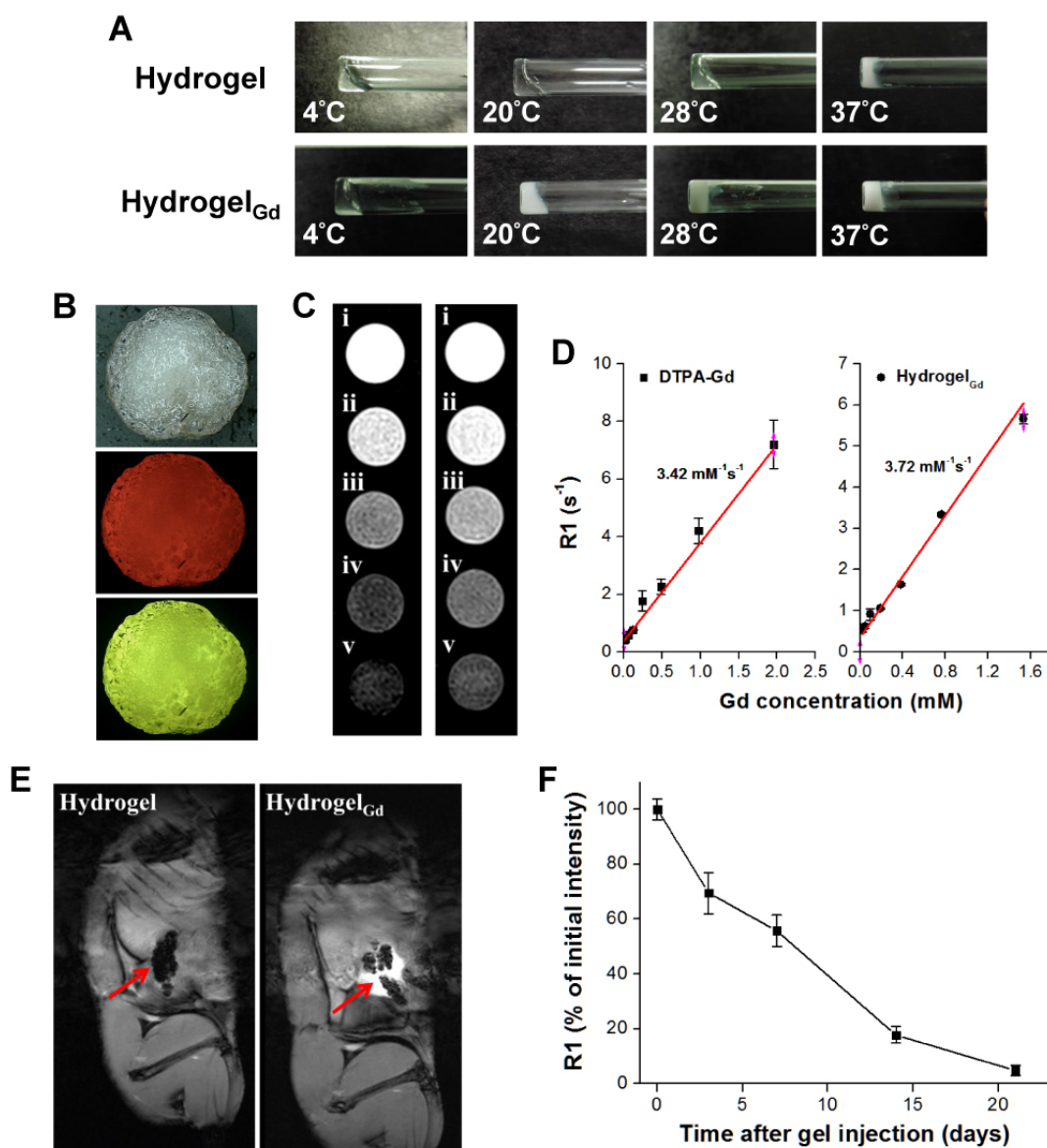


Figure 2. (A) Morphology of hydrogel and hydrogel_{Gd} (20 wt%) incubated at different temperatures. (B) Pictures of BSA/PTX NPs incorporated hydrogel_{Gd}/EPI formation. Red fluorescence: EPI; green fluorescence: FITC-labeled BSA NPs. (C) MR T1 phantom imaging of (left) commercial DTPA-Gd (i: 1.96 mM; ii: 0.98 mM; iii: 0.48 mM; iv: 0.24 mM; v: 0.12 mM) and (right) hydrogel_{Gd} (i: 1.56 mM; ii: 0.78 mM; iii: 0.40 mM; iv: 0.20 mM; v: 0.10 mM). (D) MR T1 relaxivities of (left) DTPA-Gd and (right) hydrogel_{Gd} (mM⁻¹s⁻¹) are indicated by the slope. (E) Typical MR contrast-enhanced T1 images of (left) hydrogel and (right) hydrogel_{Gd} implanted in tumor-bearing mice. (F) The reduction of MR T1 intensity of BSA NPs-incorporated hydrogel_{Gd} in tumor site. Values are means \pm SD (n = 3).

Properties of MR imaging

The BSA NPs incorporated hydrogel_{Gd} exhibited strong MR T1-weighted contrast ability at 7-T MR scanner that is similar with commercial MR T1 contrast agent (DTPA-Gd) (Figure 2C). The R1 relaxivity of the BSA NPs incorporated hydrogel_{Gd} was determined to be $3.72 \text{ mM}^{-1} \text{ s}^{-1}$ at 7-T MR scanner and exhibited an obvious trend of T1 positive contrast with the increase of gadolinium content, while there was a little stronger T1 positive contrast than commercial DTPA-Gd ($3.42 \text{ mM}^{-1} \text{ s}^{-1}$), both has high correlation ratio ($r^2 = 0.981$ for DTPA-Gd; $r^2 = 0.989$ for hydrogel_{Gd}) (Figure 2D). Next, we also investigated the MR T1 contrast ability and intratumoral distribution of BSA NPs incorporated hydrogel_{Gd} in tumors (Figure 2E). The tumor sites after the BSA NPs incorporated hydrogel_{Gd} implantation exhibited characteristically bright in T1 images compared to control group (post-implantation of BSA NPs incorporated hydrogel). The signal intensity started to reduce gradually up to 21 days after injection, caused by slow degradation and removal of BSA NPs incorporated hydrogel_{Gd} from tumor sites (Figure 2F). To summarize, we can easily monitor the BSA NPs incorporated hydrogel_{Gd} how long would be degraded and how distributed in tumor tissues using MR imaging.

Drug encapsulation and release studies

Hydrogel is the water content material that is difficult to entrap the hydrophobic PTX. Thus, the PTX was first encapsulated in BSA NPs to form BSA/PTX NPs then loaded into the hydrogel_{Gd} with hydrophilic EPI together to form BSA/PTX NPs incorporated hydrogel_{Gd}/EPI. The diameter of BSA NPs was increased to $181.7 \pm 3.9 \text{ nm}$ from $148.8 \pm 4.7 \text{ nm}$ and the surface became rough after PTX encapsulation measured by ZetaSizer (NanoPartica SZ-100Z, Horiba Instruments, Kyoto, Japan) and transmission electron microscopy (TEM) (Figure S5A), indicating the PTX was entrapped in BSA NPs and some adsorbed on their surface. It also was confirmed by FTIR, the characteristic bands present in BSA NPs are Amide I at 1655 cm^{-1} , Amide II band at 1539 cm^{-1} and Amide III region at 1240 cm^{-1} [23]. Additional peak corresponding to the ν of C-O-C (1111 cm^{-1}) for PTX exhibited in BSA/PTX NPs (Figure S5B) [30]. The amount of PTX entrapped in BSA NPs increased as the weight ratio of PTX to BSA increased, reaching a maximum concentration of $62.5 \pm 3.3 \text{ }\mu\text{g}/160 \text{ }\mu\text{g}$ NPs with an encapsulation efficiency (EE) of $41.6 \pm 2.2\%$ (Figure 3A). However, the loading efficiency (LE) reached to the maximum ($39.1 \pm 2.2\%$) at this condition (Figure 3B) that was a little higher than the previous report of Sadeghi *et al.* (around 20%)

[31]. A maximum concentration of EPI ($492.8 \pm 65.6 \text{ }\mu\text{g}$ in $10 \text{ }\mu\text{L}$ hydrogel_{Gd}) with a LE of $82.1 \pm 5.5\%$ was co-entrapped with constant BSA/PTX NPs (containing $100 \text{ }\mu\text{g}$ PTX) in hydrogel_{Gd} (Figure 3C), that was higher than the entrapment of EPI only ($391.8 \pm 73.7 \text{ }\mu\text{g}$ in $10 \text{ }\mu\text{L}$ hydrogel_{Gd}) with a LE of $65.3 \pm 6.1\%$ (Figure 3D), most likely the some of the EPI (positive charge) was also adsorbed on the surface of BSA/PTX NPs (negative charge) during the entrapment process. The results indicated that the BSA NPs incorporation cannot only used to deliver hydrophobic PTX but also significantly enhance the loading concentration of EPI in hydrogel_{Gd} to show the remarkable tumor inhibition.

Another important point would affect the therapeutic efficiency is drug released ratio and period. The EPI was rapidly released from hydrogel (without DTPA_{Gd}/bPEI addition) over 90% in 48 h. Conversely, the released rate was significantly slowed down after addition of DTPA_{Gd}/bPEI, as the ratio of DTPA_{Gd}/bPEI increased, the relative released rate of EPI decreased. For the ratio of 5:1 (CMC-g-PNIPAAmMA:DTPA_{Gd}/bPEI), it needed about 54.4 h to release 50% of EPI that was further prolonged to 97.5 h while the ratio changed to 2:1 at pH 7.4 and 37°C (Figure 4A). After that, additional 31.1% of EPI was continuously released from the hydrogel_{Gd} (ratio = 2:1) till 264 h of incubation; the maximum EPI (78.9%) was released from the hydrogel_{Gd} (ratio = 5:1) after 120 h of incubation. The results demonstrated more DTPA_{Gd}/bPEI would link the molecule chains of CMC-g-PNIPAAmMA tighter to reduce the level of swelling, resulting in longer drug release period. For the purpose of the long-term drug release, we prepared the hydrogel_{Gd} using the ratio of 2:1 in this study. That also confirmed by morphology change using scanning electron microscope (SEM), the hydrogel_{Gd} swelled and degraded to produce pores after incubation then the phenomenon became to be more obvious with increasing incubation time to 14 days (Figure S6). For BSA/PTX NPs incorporated hydrogel_{Gd}/EPI, the 50% of EPI was released from hydrogel_{Gd} after 116.8 h of incubation that longer than EPI-only entrapped hydrogel_{Gd} (97.5 h), likely some of EPI was adsorbed on the surface of BSA/PTX NPs resulted in the lag of EPI release. Moreover, longer incubation time (274.6 h) was required to release 50% of PTX from hydrogel_{Gd} and BSA NPs then kept releasing to reach maximum release ratio ($67.7 \pm 3.8\%$) after 408 h of incubation (Figure 4B). The results demonstrated this synergistic delivery system could sustainably release EPI and PTX in chronological order for preventing tumor recurrence.

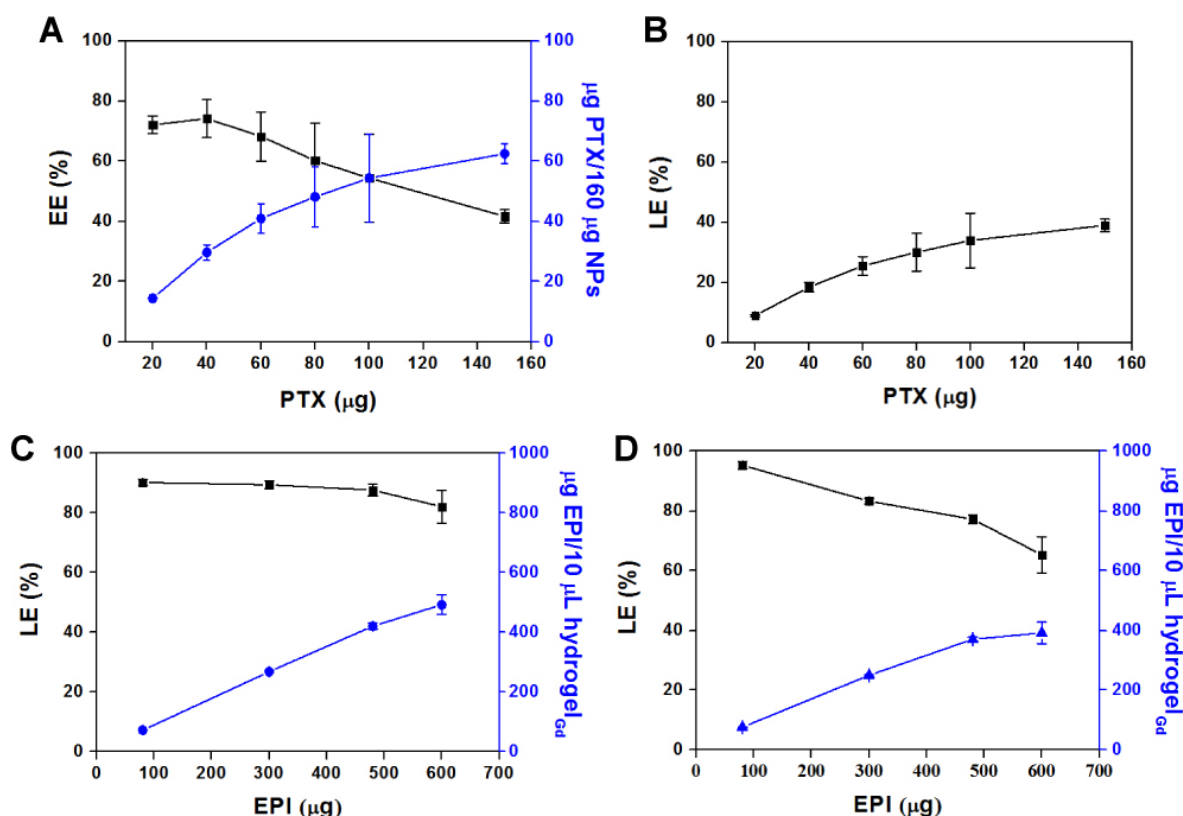


Figure 3. (A) Amount of PTX entrapped per 160 μg of BSA NPs vs. amount of PTX added, and its encapsulation efficiency (EE%). (B) The loading efficiency (LE%) in NPs. Values are means \pm SD ($n = 3$). (C) Amount of EPI entrapped per 10 μL of BSA/PTX NPs incorporated hydrogel_{Gd} vs. amount of EPI added, and its loading efficiency (LE%). (D) Amount of EPI entrapped per 10 μL of hydrogel_{Gd} vs. amount of EPI added, and its loading efficiency (LE%). Values are means \pm SD ($n = 3$).

The sustained drug release behavior of BSA/PTX NPs incorporated hydrogel_{Gd}/EPI in MBR 614 cells was also investigated, the fluorescein isothiocyanate (FITC) was used to replace the PTX for convenient detection and quantification. When MBR 614 cells were treated with free EPI at 37°C for 3 h, rapid EPI accumulation (red fluorescence) in the cell cytoplasm and nuclei was observed to initiate the cell death pathway; then the accumulated EPI in cells significantly increased at 10th h (Figure 4C). On the contrary, only a little EPI was observed in cells released from hydrogel_{Gd} (no green fluorescence exhibition) after 3 h of incubation then gradually increased with increasing the incubation time. Week green fluorescence was observed in the cells after 10 h of incubation, indicating the release rate of BSA NPs from hydrogel_{Gd} was slower than EPI (Figure 4D). Most likely the molecule chains of CMC-g-PNIPAAmMA still linked tightly with DTPA_{Gd}/bPEI that did not allow the escape of BSA NPs with a bigger size than EPI at this time point. The results showed that BSA/PTX NPs incorporated hydrogel_{Gd}/EPI could sustainably release hydrophilic (EPI) and hydrophobic (PTX) drugs stage-by-stage to effectively inhibit the residual tumor cells after post-operation of brain tumor.

In vitro cytotoxicity studies

Moreover, the BSA NPs incorporated hydrogel_{Gd} has been proved to be innocuous for the use in organisms by the *in vitro* hemolysis and cell studies (Figure S7). The BSA NPs incorporated hydrogel_{Gd} did not cause any hemolysis in mouse erythrocyte compared with the positive control group (DI-water) by spectral analysis even at high concentration (24 wt%). The cell viability was also not significantly affected compared to the untreated group even at 360 $\mu\text{g}/\text{mL}$ of BSA NPs incorporated with 10.5 mg/mL of hydrogel_{Gd} (Figure S8). The results showed that BSA NPs incorporated hydrogel_{Gd} has no obvious hemolytic activity and toxicity towards the cells.

The anti-proliferation of BSA/PTX NPs incorporated hydrogel_{Gd}/EPI toward MBR 614 cells was evaluated using the 2,3-bis-(2-methoxy-4-nitro-5-sulfophenyl)-2H-tetrazolium-5-carboxanilide (XTT) assay (Figure 5A). Free EPI showed remarkably higher treatment efficacy when used to treat MBR 614 cells with low IC₅₀ (i.e., the concentration required for 50% inhibition of cellular growth) value as 1.62 $\mu\text{g}/\text{mL}$, indicating its huge toxicity could rapidly kill the cells but also induce significantly side-effect for normal tissues. Moreover, the IC₅₀ significantly

increased to 19.94 $\mu\text{g}/\text{mL}$ while the MBR 614 cells were incubated with hydrogel_{Gd}/EPI, most likely only few EPI ($7.8 \pm 0.9\%$) could be released from hydrogel_{Gd} within 24 h that has been proved in drug release study. In addition, IC₅₀ was not remarkably reduced (13.46 $\mu\text{g}/\text{mL}$) while MBR 614 cells treated with BSA/PTX NPs incorporated hydrogel_{Gd}/EPI (containing 10 $\mu\text{g}/\text{mL}$ PTX) because only a little PTX was released from hydrogel_{Gd} and BSA NPs at this time point. When the cells incubated with BSA/PTX NPs incorporated hydrogel_{Gd}/EPI for 48 h, the IC₅₀ was further remarkably reduced to 0.85 $\mu\text{g}/\text{mL}$, indicating that more EPI ($18.6 \pm 1.8\%$ from $6.4 \pm 1.1\%$) and PTX ($4.6 \pm 0.9\%$ from $1.4 \pm 0.4\%$) has been released from hydrogel_{Gd} to synergistically inhibit the tumor cells with highly controlled treatment efficacy.

In vivo anti-proliferation efficiency

To confirm the BSA NPs incorporated hydrogel_{Gd} would not induce the apoptosis toward tissues, the tissues were stained Caspase-3 antibody after 7 days of injection with BSA NPs incorporated hydrogel_{Gd}. We did not find the significant active Caspase-3 in BSA NPs incorporated hydrogel_{Gd} injected skin tissues compared to no treated tissues, indicating that the formulation of BSA NPs incorporated hydrogel_{Gd} would not induce any apoptosis effects (Figure 5B, C). Next, we resected a portion of the xenograft tumor in MBR 614 tumor-bearing mice then spread the BSA/PTX NPs incorporated hydrogel_{Gd}/EPI (containing 1 mg of EPI and 0.1 mg of PTX) in the cavity immediately. BSA/PTX NPs incorporated hydrogel_{Gd}/EPI exhibited significant inhibition of the tumor growth rate compared to the control group (saline), BSA NPs incorporated hydrogel_{Gd} (without any drugs), and free EPI (via i.v. injection) groups (Figure 6A). The BSA/PTX NPs incorporated hydrogel_{Gd}/EPI appear to show the synergistic therapeutic and sustained drug release effects of using EPI and BSA/PTX NPs incorporation, which were kept as constant concentration till two-week by controlled release. After 14 days, the groups treated with saline and BSA NPs incorporated hydrogel_{Gd} showed no tumor regression then continuous tumor growth (saline: 1827.3 ± 543.2 from 67.9 ± 13.2 mm^3 ; BSA NPs incorporated hydrogel_{Gd}: 1421.5 ± 550.7 from 60.6 ± 34.7 mm^3). The tumor growth rates were slightly suppressed in the free EPI treated group (654.9 ± 250.7 from 61.6 ± 30.3 mm^3) but the tumors progressed rapidly after 18 days of treatment, in which free EPI accumulate non-specifically at the tumor sites resulting in low drug concentration in tumor tissues. In contrast, BSA/PTX NPs incorporated hydrogel_{Gd}/EPI showed remarkable tumor growth

suppression over 63 days without the phenomenon of tumor recurrence, most likely the EPI was released from hydrogel_{Gd} at first stage to inhibit the tumor progression then the tumor was continuously inhibited and cured by the following released PTX from hydrogel_{Gd} and BSA NPs at second stage. Importantly, average survival was significantly improved in mice receiving BSA/PTX NPs incorporated hydrogel_{Gd}/EPI treatment to outclass 63 days of median survival, compared to average survival spans of only about 18 days for control group, 21 days for BSA incorporated hydrogel_{Gd} treated group, and 32 days for free EPI treated group (Figure 6B). Most notably, there was no significant loss of body weight in mice receiving either BSA NPs incorporated hydrogel_{Gd} or BSA/PTX NPs incorporated hydrogel_{Gd}/EPI (Figure S9A). Photographs of mice confirmed that treatment with BSA/PTX NPs incorporated hydrogel_{Gd}/EPI was significantly more effective for tumor reduction and recurrence prevention compared to other groups (Figure S10).

We also did the human glioma U87 tumor-bearing mouse model to reconfirm the ability of tumor inhibition of BSA/PTX NPs incorporated hydrogel_{Gd}/EPI, the experimental protocols and conditions were same as above mentioned. The mice treated with BSA NPs incorporated hydrogel_{Gd} showed no tumor inhibition effect same as control group after 23 days of treatment (control: 2591.5 ± 787.4 from 157.8 ± 42.9 mm^3 ; BSA NPs incorporated hydrogel_{Gd}: 3112.7 ± 90.8 from 192.3 ± 61.3 mm^3). The tumor growth rates were slightly suppressed in the BSA/PTX NPs incorporated hydrogel_{Gd} treated group, most likely the PTX cannot promptly be released from hydrogel_{Gd} and BSA NPs (only 15% of PTX was released at first 100 h) to inhibit the rapid growth of tumor. Conversely, the hydrogel_{Gd}/EPI showed more efficient to inhibit tumor progression due to the about 50% of EPI could be released at first 100 h to inhibit the tumor growth rate than another 30% could be further gradually released to keep the reduction of tumor growth rate. Interestingly, BSA/PTX NPs incorporated hydrogel_{Gd}/EPI showed remarkable tumor growth suppression over 69 days without the phenomenon of tumor recurrence, most likely the EPI was released from hydrogel_{Gd} at first stage to inhibit the tumor progression then the tumor was continuously inhibited and cured by the following released PTX from hydrogel_{Gd} and BSA NPs at second stage (Figure 6C). Importantly, average survival was significantly improved in mice receiving BSA/PTX NPs incorporated hydrogel_{Gd}/EPI treatment to outclass 69 days of median survival, compared to average survival spans of only about 27

days for control and BSA NPs incorporated hydrogel_{Gd} treated groups, 34 days for BSA/PTX NPs incorporated hydrogel_{Gd} treated group, 48 days for hydrogel_{Gd}/EPI treated group (Figure 6D). No significant loss of body weight in treated mice was observed (Figure S9B). The results demonstrated the potency of the therapeutic strategy of effective dose delivery and sustained release that was successfully developed to inhibit the tumor progression and prevent the recurrence in this study.

Conclusion

In conclusion, we have successfully upgraded PNIPAAm-based hydrogel to be MRI traceable and rapid gelation hydrogel as dual-drug delivery system (incorporation of BSA/PTX NPs and EPI) to prevent the post-operative recurrence of brain tumor. BSA/PTX NPs incorporated hydrogel_{Gd}/EPI exhibit the following beneficial features: i) ultrahighly

thermosensitive with low LCST, resulting in the rapid solidification at 28°C in 4 sec which is suitable for use in operation room; ii) co-delivery hydrophilic and hydrophobic drugs by BSA/PTX NPs incorporation system that also exhibits controlled release with long-term period stage by stage; iii) high MR T1 contrast ability of hydrogel_{Gd} resulting in a real-time monitor of the hydrogel degradation and distribution in tumor tissues; iv) high efficiency for tumor inhibition and recurrence prevention after surgical operation. Our synergistic strategy presents a conceptually new approach to the development of locally and long-termly drug release system against brain tumor recurrence used for post-operation. We believe that these unique features of BSA/PTX NPs incorporated hydrogel_{Gd}/EPI make the nanocomposite design described herein an ideal starting point for further developments in therapeutic dosing schedule-dictating nanocomposites.

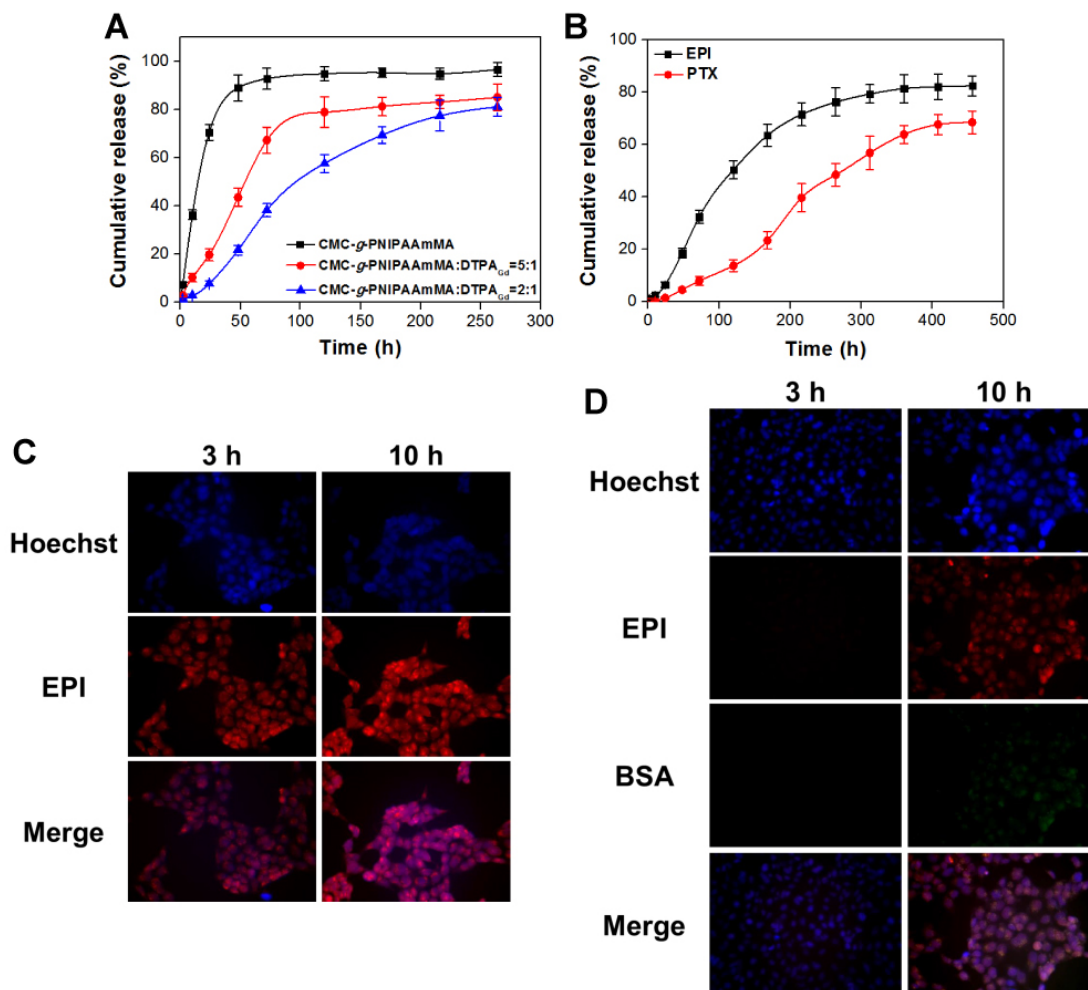


Figure 4. (A) *In vitro* release profiles of EPI from hydrogel (CMC-g-PNIPAAmMA) and hydrogel_{Gd} (blends of CMC-g-PNIPAAmMA and DTPA_{Gd}/bPEI with different ratios) in PBS (pH 7.4) at 37°C. Values are means ± SD (n = 3). (B) *In vitro* release profiles of EPI and PTX from BSA/PTX NPs incorporated hydrogel_{Gd}/EPI (CMC-g-PNIPAAmMA:DTPA_{Gd}/bPEI = 2:1) in PBS (pH 5.6) at 37°C. Values are means ± SD (n = 3). (C) The fluorescence imaging of MBR 614 cells treated with free EPI (5 µg/mL) at 37°C for 3 or 10 h. (D) The fluorescence imaging of MBR 614 cells treated with BSA/FITC incorporated hydrogel_{Gd}/EPI (5 µg/mL) at 37°C for 3 or 10 h. (red color: EPI; green color: BSA/FITC NPs; blue color: nuclei).

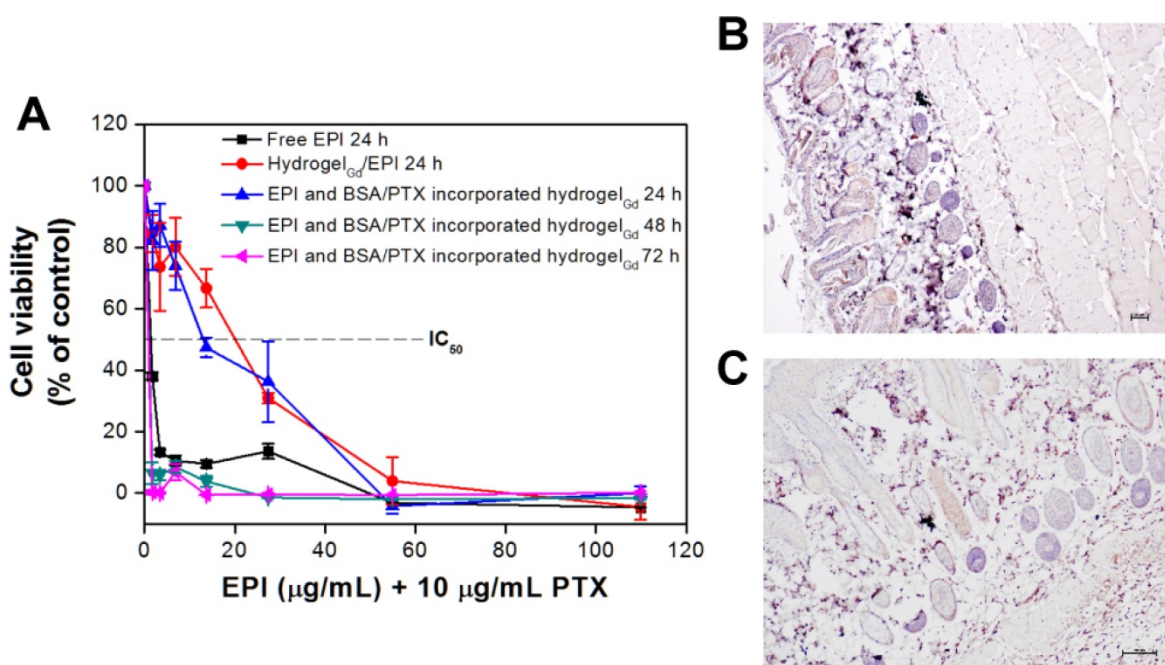


Figure 5. (A) *In vitro* anti-proliferation of MBR 614 cells after treatment with different samples with various EPI concentrations for 24, 48, or 72 h. Values are the means \pm S.D. (n = 6). IHC on paraffin sections of mouse skin for apoptosis staining by detection of active caspase-3 (B) normal mouse skin without treatment and (C) normal mouse skin with BSA NPs incorporated hydrogel_{Gd} injection.)

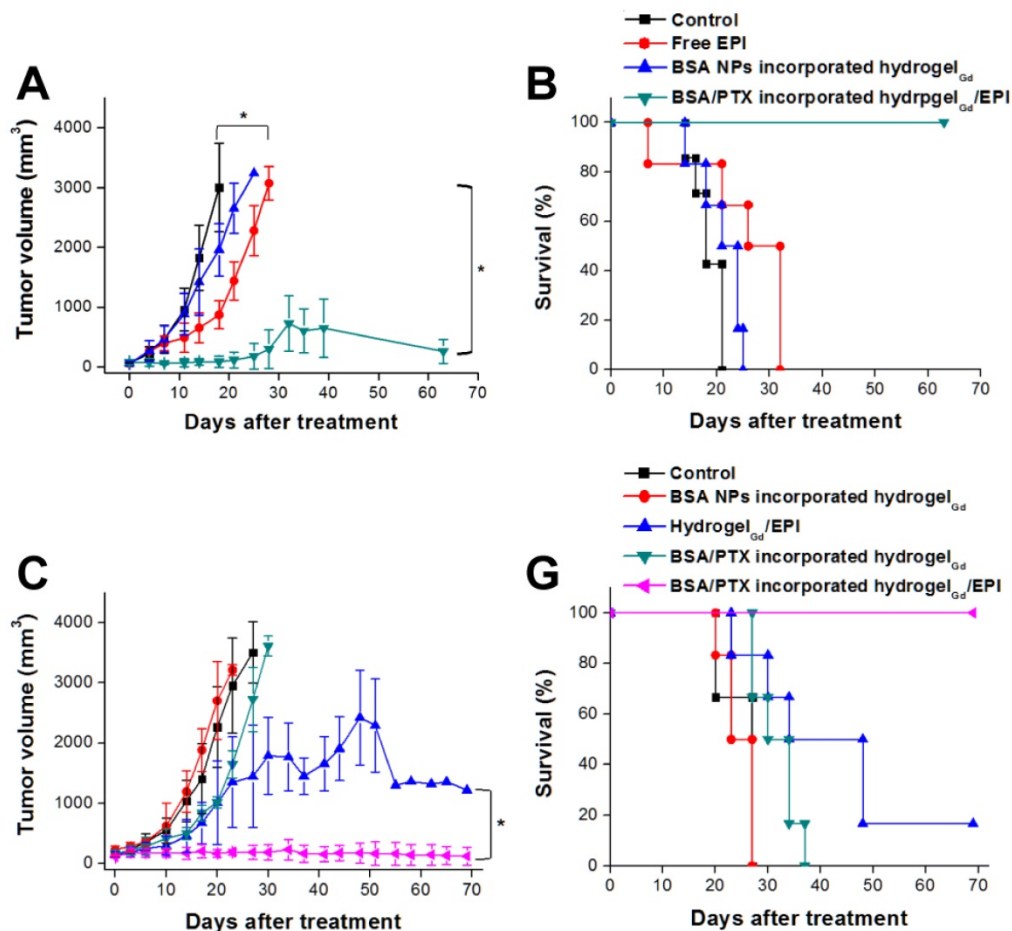


Figure 6. (A) Tumor growth curves of mice bearing MBR 614 tumors after surgical operation then treatment with free EPI (i.v. injection) or BSA NPs incorporated hydrogel_{Gd} implantation or BSA/PTX NPs incorporated hydrogel_{Gd}/EPI implantation. Values are the means \pm S.D. (n = 6). (B) Survival curves of mice bearing MBR 614 tumors after different treatments. Values are the means \pm S.D. (n = 6). (C) Tumor growth curves of mice bearing U87 tumors after surgical operation then treatment with BSA NPs incorporated hydrogel_{Gd} or hydrogel_{Gd}/EPI or BSA/PTX NPs incorporated hydrogel_{Gd} or BSA/PTX NPs incorporated hydrogel_{Gd}/EPI implantation. Values are the means \pm S.D. (n = 6). (D) Survival curves of mice bearing U87 tumors after different treatments. Values are the means \pm S.D. (n = 6).

Acknowledgment

We thank the Ministry of Science and Technology, Chang Gung Memorial Hospital, and National Health Research Institutes, Taiwan (R.O.C.), for the financial assistance provided (MOST103-2320-B-110-004-MY2, MOST105-2314-B-110-001, CMRPG3F1731, CIRPG3E2041, and NHRI-EX106-10502NI). We would also like to thank Ms. Li-Ying Feng, Chang Gung Memorial Hospital Microscopy Core Laboratory, and Center for Advanced Molecular Imaging and Translation for assistance with Immunohistochemistry, TEM, and MRI.

Supplementary Material

Supplementary figures and table (Figures S1–S10 and table S1). <http://www.thno.org/v07p2524s1.pdf>

Competing Interests

The authors have declared that no competing interest exists.

References

- Kim GY, Tyler BM, Tupper MM, et al. Resorbable polymer microchips releasing BCNU inhibit tumor growth in the rat 9L flank model. *J Control Release*. 2007; 123: 172–8.
- Stupp R, Mason WP, Bent MJ, et al. Radiotherapy plus concomitant and adjuvant temozolomide for glioblastoma. *N Engl J Med*. 2005; 352: 987–96.
- Pardridge WM. The blood-brain barrier and neurotherapeutics. *NeuroRx*. 2005; 2: 1–2.
- Dixit S, Novak T, Miller K, et al. Transferrin receptor-targeted theranostic gold nanoparticles for photosensitizer delivery in brain tumors. *Nanoscale*. 2015; 7: 1782–90.
- Qiao R, Jia Q, Hüwel S, et al. Receptor-mediated delivery of magnetic nanoparticles across the blood–brain barrier. *ACS Nano*. 2012; 6: 3304–10.
- Westphal M, Hill DC, Bortey E, et al. A phase 3 trial of local chemotherapy with biodegradable carmustine (BCNU) wafers (Gliadel Wafers) in patients with primary malignant glioma. *Neuro Oncol*. 2003; 5: 79–88.
- Valtonen S, Timonen U, Toivanen P, et al. Interstitial chemotherapy with carmustine-loaded polymers for high-grade gliomas: a randomized double-blind study. *Neurosurgery*. 1997; 41: 44–8.
- Fung LK, Ewend MG, Sills A, et al. Pharmacokinetics of interstitial delivery of carmustine, 4-hydroperoxycyclophosphamide, and paclitaxel from a biodegradable polymer implant in the monkey brain. *Cancer Res*. 1998; 58: 672–84.
- Liu HL, Hua MY, Yang HW, et al. Magnetic resonance monitoring of focused ultrasound/magnetic nanoparticle targeting delivery of therapeutic agents to the brain. *Proc Natl Acad Sci U.S.A.* 2010; 107: 15205–10.
- Fan CH, Ting CY, Lin HJ, et al. SPIO-conjugated, doxorubicin-loaded microbubbles for concurrent MRI and focused-ultrasound enhanced brain-tumor drug delivery. *Biomaterials*. 2013; 34: 3706–15.
- Allard E, Passirani C, Benoit JP. Convection-enhanced delivery of nanocarriers for the treatment of brain tumors. *Biomaterials*. 2009; 30: 2302–18.
- Appel EA, Barrio J del, Loh XJ, et al. Supramolecular polymeric hydrogels. *Chem Soc Rev*. 2012; 41: 6195–214.
- Lutolf MP, Hubbell JA. Synthetic biomaterials as instructive extracellular microenvironments for morphogenesis in tissue engineering. *Nat Biotechnol*. 2005; 23: 47–55.
- Bai H, Li C, Wang X, et al. A pH-sensitive graphene oxide composite hydrogel. *Chem Commun*. 2010; 46: 2376–8.
- Ma X, Li Y, Wang W, et al. Temperature-sensitive poly(N-isopropylacrylamide)/graphene oxide nanocomposite hydrogels by in situ polymerization with improved swelling capability and mechanical behavior. *Eur Polym J*. 2013; 49: 389–96.
- Kharkar PM, Kiick KL, Kloxin KM. Design of thiol- and light-sensitive degradable hydrogels using Michael-type addition reactions. *Polym Chem*. 2015; 6: 5565–74.
- Jin S, Gu J, Shi Y, et al. Preparation and electrical sensitive behavior of poly(N-vinylpyrrolidone-co-acrylic acid) hydrogel with flexible chain nature. *Eur Polym J*. 2013; 49: 1871–80.
- Boffito M, Sirianni P, Rienzo AMD, et al. Thermosensitive block copolymer hydrogels based on poly(ϵ -caprolactone) and polyethylene glycol for biomedical applications: State of the art and future perspectives. *J Biomed Mater Res A*. 2015; 103: 1276–90.
- Jhan HJ, Liu JJ, Chen YC, et al. Novel injectable thermosensitive hydrogels for delivering hyaluronic acid–doxorubicin nanocomplexes to locally treat tumors. *Nanomedicine*. 2014; 10: 1–12.
- Elstad NL, Fowers KD. OncoGel (ReGel/paclitaxel) – Clinical applications for a novel paclitaxel delivery system. *Adv Drug Deliver Rev*. 2009; 61: 785–94.
- Zhang XZ, Yang YY, Chung TS, et al. Preparation and characterization of fast response macroporous poly(N-isopropylacrylamide) hydrogels. *Langmuir*. 2001; 17: 6094–9.
- Zu Y, Zhang Y, Zhao X, et al. Optimization of the preparation process of vinblastine sulfate (VBLs)-loaded folateconjugated bovine serum albumin (BSA) nanoparticles for tumor-targeted drug delivery using response surface methodology (RSM). *Int J Nanomedicine*. 2009; 4: 321–33.
- Sripriyalakshmi S, Anjali CH, George PD, et al. BSA nanoparticle loaded atorvastatin calcium—a new facet for an old drug. *PLOS ONE*. 2014; 9: e86317.
- Karmali PP, Kotamraju VR, Kastantin M, et al. Targeting of albumin-embedded paclitaxel nanoparticles to tumors. *Nanomedicine*. 2009; 5: 73–82.
- Turturro SB, Guthrie MJ, Appel AA, et al. The effects of cross-linked thermo-responsive PNIPAAm-based hydrogel injection on retinal function. *Biomaterials*. 2011; 32: 3620–6.
- Vandervoort J, Ludwig A. Preparation and evaluation of drug-loaded gelatin nanoparticles for topical ophthalmic use. *Eur J Pharm Biopharm*. 2004; 57: 251–61.
- Hori K, Sotozono C, Hamuro J, et al. Controlled release of epidermal growth factor from cationized gelatin hydrogel enhances corneal epithelial wound healing. *J Control Release*. 2007; 118: 169–76.
- Lai JY, Hsieh AC. A gelatin-g-poly(N-isopropylacrylamide) biodegradable in situ gelling delivery system for the intracameral administration of pilocarpine. *Biomaterials*. 2012; 33: 2372–87.
- Adel AM, Abou-Youssef H, El-Gendy AA, et al. Carboxymethylated cellulose hydrogel; sorption behavior and characterization. *Nature and Science*. 2010; 8: 244–56.
- Hua MY, Yang HW, Chuang CK, et al. Magnetic-nanoparticle-modified paclitaxel for targeted therapy for prostate cancer. *Biomaterials*. 2010; 31: 7355–63.
- Sadeghi R, Moosavi-Movahedi AA, Emam-jomeh Z, et al. The effect of different desolvating agents on BSA nanoparticle properties and encapsulation of curcumin. *J Nanopart Res*. 2014; 16: e2565.